HHS Public Access

Author manuscript

J Bone Miner Res. Author manuscript; available in PMC 2021 October 29.

Published in final edited form as:

J Bone Miner Res. 2020 June ; 35(6): 1188–1202. doi:10.1002/jbmr.3987.

Glucocorticoids Disrupt Skeletal Angiogenesis Through Transrepression of NF-κB–Mediated Preosteoclast *Pdgfb* Transcription in Young Mice

Yi Peng[1,2], **Shan Lv**[2,3], **Yusheng Li**[4], **Jianxi Zhu**[2,3], **Shijie Chen**[1], **Gehua Zhen**[2], **Xu Cao**[2], **Song Wu**[1], **Janet L. Crane**[2,5]

[1]Department of Orthopedic Surgery, The Third Xiangya Hospital, Central South University, Changsha, China

[2]Department of Orthopedic Surgery, The Johns Hopkins University School of Medicine, Baltimore, MD, USA

[3]Geriatric Endocrinology, The First Hospital Affiliated to Nanjing Medical University, Nanjing, China

[4]Department of Orthopedic Surgery, Xiangya Hospital of Central South University, Changsha, China

[5]Department of Pediatrics, The Johns Hopkins University School of Medicine, Baltimore, MD, USA

Abstract

In the growing skeleton, angiogenesis is intimately coupled with osteogenesis. Chronic, high doses of glucocorticoids (GCs) are associated with decreased bone vasculature and induce osteoporosis and growth failure. The mechanism of GC-suppression of angiogenesis and relationship to osteoporosis and growth retardation remains largely unknown. Type H vessels, which are regulated by preosteoclast (POC) platelet-derived growth factor–BB (PDGF-BB), are specifically coupled with bone formation and development. We determined the effect of GCs on POC synthesis of PDGF-BB in relation to type H vessel formation, bone mass, and bone growth in the distal femur of 2-week-old young mice receiving prednisolone or vehicle for 2, 4, or 6 weeks. After 2 weeks of prednisolone, the number of POCs were unchanged while POC synthesis of PDGF-BB was reduced. Longer treatment with prednisolone reduced POCs numbers and PDGF-BB. These changes were associated with a reduction in type H vessels, bone formation rate, bone mass, and bone length at each time point. In vitro, excessive concentrations of prednisolone (10^{-6}M) resulted in decreased PDGF-BB concentration and POC numbers. Conditioned medium from POC cultures treated with control concentration of prednisolone (10^{-7}M) or recombinant PDGF-BB stimulated endothelial tube formation, whereas conditioned medium from control concentration of

Address correspondence to: Janet L Crane, MD, Johns Hopkins University, 200 N Wolfe St, Rm 3120, Baltimore, MD 21287, USA. jcrane2@jhmi.edu.

Disclosures

All authors declare that they have no conflict of interests.

Additional Supporting Information may be found in the online version of this article.

The peer review history for this article is available at https://publons.com/publon/10.1002/jbmr.3987.

prednisolone-treated POC cultures neutralized by PDGF-BB antibody or excessive prednisolone inhibited endothelial tube formation. Administration of excessive prednisolone attenuated the P65 subunit of nuclear factor kappa B (NF-κB) binding to the *Pdgfb* promoter, resulting in lower *Pdgfb* transcription. Co-treatment with excessive prednisolone and the glucocorticoid receptor (GR) antagonist (RU486), GR siRNA, or TNFα rescued NF-κB binding to the *Pdgfb* promoter and endothelial tube formation. These results indicate that PDGF-BB synthesis in POCs is suppressed by GCs through transrepression of GR/NF-κB, thus inhibiting type H vessel formation and associated osteoporosis and growth failure.

Keywords

ANGIOGENESIS; BONE LOSS; GLUCOCORTICOIDS; GROWTH FAILURE; NF-κB; OSTEOGENESIS; OSTEOPOROSIS; PDGF-BB; TYPE H VESSELS

Introduction

Glucocorticoids (GCs) are widely used to treat various inflammatory and autoimmune disorders in childhood, such as muscular dystrophy, juvenile rheumatoid arthritis, inflammatory bowel disease, leukemia, kidney disease, and asthma. Approximately 10% of children receive GC therapy.[1] Long-term use of GCs results in irreversible effects on bone health including bone loss and growth retardation.[2,3] Currently, there are no US Food and Drug Administration (FDA)-approved treatments to combat osteotoxic effects of GCs in childhood, in part because its pathogenesis is incompletely understood. There have been extensive studies about GC effects on the bone in the mature skeleton, particularly osteoclasts and osteoblasts. In the growing skeleton, however, knowledge gaps still exist, which limits clinical care. Bone, particularly growing bone, is highly vascularized. Vasculature plays a critical role in maintaining bone homeostasis, not only for their conventional role in providing bone cells with nutrients, growth factors, and hormones, but also for their active role in regulating bone formation.[4] In the growing skeleton, angiogenesis is temporally and spatially coupled with osteogenesis.[5,6] GCs are known to inhibit angiogenesis,[7–10] but the mechanism underlying GC suppression of angiogenesis in relation to bone loss and growth retardation remains unknown.

Type H vessels, defined by high immunofluorescence for CD31 and endomucin ($CD31^{hi}Emcn^{hi}$), are found abundantly in the metaphysis adjacent to the growth plate and are associated with bone formation.[11–13] Preosteoclasts (POCs), the immature progenitors of bone-degrading osteoclasts, promote angiogenesis of type H vessels and osteogenesis during bone modeling and remodeling through the release of platelet-derived growth factor–BB (PDGF-BB).[14,15] Excessive GCs are known to inhibit osteoclastogenesis and decrease POCs,[16] suggesting that GCs may impact angiogenesis through inhibition of osteoclast-angiogenesis coupling factors.

GCs bind to the glucocorticoid receptor (GR) in the cytoplasm, which forms the GC/GR complex and translocate into the nucleus to regulate transcription of genes. Previous studies have suggested that nuclear factor kappa-light-chain-enhancer of activated B cells (NF-κB) signaling pathway is associated with PDGF-BB production[17,18] and is necessary for

induction of PDGF-BB expression of NF-κB.[19] Because GC/GR transrepression effects can be mediated by NF-κB or activator protein 1 (AP-1),[20] we explored the NF-κB pathway as a potential mechanism of GC-suppression of PDGF-BB. Specifically, we investigated the effect of GCs on PDGF-BB synthesis in POCs and the relationship to GC-suppression of angiogenesis, bone loss, and growth retardation. We determined that the mechanism of GC suppression of PDGF-BB secretion in POCs was via the GR/NF-κB signaling pathway, which resulted in suppression of type H vessel formation and was associated with bone loss and growth retardation.

Materials and Methods

Animals

We modified our young GC-osteotoxic mouse model[9] using a higher dose of prednisolone (20 mg/m^2/day). Briefly, 2-week-old C57BL/6J mice were administered either phosphate-buffered saline (PBS; Gibco, Grand Island, NY, USA) or prednisolone (Sigma-Aldrich, St. Louis, MO, USA) by daily intraperitoneal injection. Each group had six males. We also examined three females per group, which had similar results (data not shown). For the prednisolone administration, body surface area ($m^2 = kW^{2/3}$, k = 9.82, W = weight (g)) was utilized rather than weight to account for the high metabolic rate in young mice and to allow direct extrapolation for comparison of the dose utilized in mice to humans.[9,21,22] Supplementary Table 1 provides conversion of dosage by body surface area versus weight. Mice were euthanized after 2, 4, and 6 weeks of prednisolone or PBS. Serum, femurs, and tibias were collected for subsequent experiments. For full details of serum and bone marrow collection and labeling for histomorphometry, please refer to the Supplementary Methods. To validate the GC suppression of *Pdgfb* is the major factor contributing to the bone vasculature phenotype, we also used *Trap-Cre*; $Pdgfb^{flox/flox}$ mice as described.[14] $Pdgfb^{flox/flox}$ mice (stock no. 017622; 129P2/OlaHsd background) were previously purchased from the Jackson Laboratory (Bar Harbor, ME, USA) and crossed with *Trap-Cre* mice obtained from J.J. Windle (Virginia Commonwealth University, Richmond, VA, USA).[23] Hemizygous TRAP-Cre mice were crossed with $Pdgfb^{flox/flox}$ mice. Offspring were intercrossed to generate *TRAP-Cre;*$Pdgfb^{-/-}$ (referred hereafter as $Pdgfb^{-/-}$) mice. $Pdgfb^{flox/flox}$ littermates were used as control. Genotypes were determined by PCR analyses of genomic DNA extracted from mouse-tail snips using the following primers: *TRAP*-Cre forward, 5′-ATATCTCACGTACTGACGGTGGG-3′ and reverse, 5′-CTGTTTCACTATCCAGGTTACGG-3′; *loxP Pdgfb* allele forward, 5′-GGGTGGGACTTTGGTGTAGAGAAG-3′ and reverse, 5′-GGAACGGATTTTGGAGGTAGTGTC-3′. Two-week-old mice ($Pdgfb^{-/-}$ or $Pdgfb^{flox/flox}$) were injected intraperitoneally daily with either vehicle or prednisolone 10 mg/m^2/day for 4 weeks, and were euthanized at 6 weeks of age. All experiments utilized six mice per group unless otherwise specified.

We maintained all animals in the Animal Facility of the Johns Hopkins University School of Medicine, housed in gangs in sterile, ventilated cages (Allentown Caging Equipment, Allentown, NJ, USA), allowed free access to water and standard mouse chow, on a 14/10 hour light/dark cycle. No adverse events occurred in the experimental animals.

The experimental protocol was reviewed and approved by the Institutional Animal Care and Use Committee of Johns Hopkins University, Baltimore, MD, USA. The Animal Facility complies with the National Institutes of Health Animal Welfare Act and maintains appropriate policies and procedures to ensure humane care and use of animals.

μCT analysis

Femora were harvested from mice with soft tissues carefully removed. Samples were fixed overnight in 4% paraformaldehyde (PFA), stored in 70% ethanol, and were scanned by high-resolution μCT (Skyscan 1172; Skyscan, Aartselaar, Belgium).[14,24] All scans were performed at a voltage of 49 kVp, current of 200 μA, and resolution of 12 μm per pixel. Image reconstruction software (NRecon v1.6; Skyscan), data analysis software (CTAn v1.9; Skyscan), and three-dimensional model visualization software (μCTVol v2.0; Skyscan) were used to analyze the parameters of the distal femoral metaphyseal trabecular bone. A trabecular bone region of interest (ROI) was drawn starting from 5% of femoral length proximal to the distal epiphyseal growth plate and extended proximally for a total of 5% of femoral length. The trabecular bone was segmented from the bone marrow and analyzed to determine the trabecular bone volume fraction (BV/TV), trabecular thickness (Tb.Th), trabecular number (Tb.N), and trabecular separation (Tb.Sp). The femoral length was determined between the femoral head and the distal metaphyseal growth plate (GP). The first crossing of the low-density cartilage structure by bone primary spongiosa was set as the reference GP level.

Histochemistry and immunostaining

Bone tissues were dissected from mice and fixed immediately in 4% PFA solution overnight, then decalcified in 0.5M EDTA with constant shaking at 4°C for 2 weeks and dehydrated in 20% sucrose and 2% polyvinylpyrrolidone (PVP) solution for 24 hours. Four-μm-thick coronal-oriented sections of the femur were processed for safranin orange and fast green staining. For tartrate resistance acid phosphatase (Trap) staining, paraffin-embedded samples were fixed, sectioned, and stained with a TRAP staining kit (Sigma-Aldrich). POCs were defined as TRAP-positive mononucleated cells, whereas osteoclasts were defined by three or more nuclei. For immunofluorescence, the bone tissues were embedded and frozen in optimal cutting temperature compound or 8% gelatin (porcine) in presence of 20% sucrose and 2% PVP. Sections were generated using low-profile blades on a Leica CM3050 cryostat (Leica Microsystems, Inc., Buffalo Grove, IL, USA). For phenotypic analysis, mutant and littermate control samples were always processed, sectioned, stained, imaged, and analyzed together at the same conditions and settings. For immunofluorescence staining, bone sections were air-dried, permeabilized for 10 min in 0.3% Triton X-100, blocked in 5% donkey serum at room temperature for 30 min, and probed with the primary antibodies diluted in 5% donkey serum in PBS overnight at 4°C. The following primary antibodies were used: Endomucin (Santa Cruz Biotechnology, Santa Cruz, CA, USA; sc-65495, 1:100), CD31 (R&D Systems, Minneapolis, MN, USA; FAB3628G, 1:100), Osterix (Abcam, Cambridge, MA, USA; ab22552, 1:100), TRAP (Abcam; ab212723, 1:400), and PDGF-BB (Abcam; ab23914, 1:50). Briefly, we incubated bone sections with individual primary antibodies to mouse. After primary antibody incubation, sections were washed with PBS three times and incubated with appropriate Alexa Fluor–coupled secondary antibodies

(Molecular Probes, Eugene, OR, USA; 1:400) for 1 hour at room temperature (RT). Nuclei were counterstained with 4,6-diamidino-2-phenylindole (DAPI). Sections were thoroughly washed with PBS before mounting using FluoroMount-G (Southern Biotech, Birmingham, AL, USA). Coverslips were sealed with nail polish.

POC culture from mouse bone marrow

Bone marrow cells were harvested from 4-week-old male wild-type mice by flushing marrow cavity from the tibia and femur and cultured with alpha minimum essential medium (α-MEM; Mediatech, Inc., Manassas, VA, USA) containing 10% fetal bovine serum (FBS), 100 U/mL streptomycin sulfate (Sigma-Aldrich) and 100 U/mL penicillin (Sigma-Aldrich) in culture dishes at 37°C in 5% CO_2 humidified incubator overnight following established protocols.[9,14] The adherent cells were discarded while the floating cells were cultured with macrophage colony-stimulating factor (M-CSF; R&D Systems; 416ML050) 30 ng/mL for 48 hours to form pure monocytes/macrophages. We also used the RAW264.7 cell line to induce preosteoclasts. To validate osteoclast differentiation, after culture with M-CSF 30 ng/mL and receptor activator of NF-κB ligand (RANKL; Abcam; ab129136) 60 ng/mL for 3 and 7 days, we stained for TRAP activity using a commercial kit (Sigma-Aldrich). All monocytes/macrophages were $Trap^+$ mononuclear cells at 3 days, whereas $Trap^+$ multinuclear cells were noted after culture for 7 days (Supplemental Fig. 1a). For POC-prednisolone studies, we added various concentration of prednisolone (0, 10^{-9}M, 10^{-8}M, 10^{-7}M, 10^{-6}M, and 10^{-5}M) to POCs to determine the effect of gradient prednisolone on POC synthesis of PDGF-BB. Once experimental and control prednisolone concentrations were determined, we added prednisolone 10^{-7}Mor 10^{-6}M alone or prednisolone 10^{-7}M plus PDGF-BB neutralizing antibodies or prednisolone 10^{-6}M plus RU486 or TNFα to POCs and cultured for 24 hours. Conditioned medium was collected from each group after centrifugation at 700*g* for 10 min at 4°C and stored at −80°C for subsequent experiments.

ELISA analysis

We examined PDGF-BB levels of serum, bone marrow supernatant, and conditioned medium using a Mouse/Rat PDGF-BB Quantikine ELISA kit (R&D Systems) according to the manufacturers' instructions.

In vitro RNA interference

For in vitro siRNA transfection, GR siRNA (Santa Cruz Biotechnology; sc-35506) and Control siRNA (Santa Cruz Biotechnology; sc-37007) were transfected into POCs according to the manufacturer's guidelines. Briefly, RAW264.7 cells were induced to differentiate into POCs by culture for 3 days in the presence of RANKL and M-CSF. POCs were transfected with either GR siRNA or control siRNA duplex diluted in siRNA transfection medium (Santa Cruz Biotechnology; sc-36868) and mixed with siRNA transfection reagent (Santa Cruz Biotechnology; sc-29528) into siRNA transfection medium after incubation for 30 min at room temperature. Cells were incubated for 6 hours at 37°C in a 5% CO_2 incubator. Transfection mixture was removed and replaced with Dulbecco's Modified Eagle Medium (DMEM) culture medium containing 10% FBS, RANKL 60 ng/mL, and M-CSF 30 ng/mL, and cells were incubated for an additional 24 hours. Conditioned medium, chromatin,

cell protein, and RNA were collected for ELISA, chromatin immunoprecipitation (ChIP), Western blot analysis, and RT-PCR.

ChIP assay

ChIP analysis was performed by using the EpiQuik™ ChIP Kit (Epigentek, Farmingdale, NY, USA). Briefly, POCs were cultured with prednisolone 10^{-6}M (with or without RU486, GRsiRNA, and TNFα) or prednisolone 10^{-7}M for 24 hours. A total of 3×10^6 POC cells of each group were cross-linked with 1% formaldehyde for 10 min at room temperature. Chromatin was extracted and sonicated to DNA fragments with a mean length of 200 to 1000 bp. Immunoprecipitation (IP) was performed for 90 min using an antibody against the p65 subunit of NF-κB (Santa Cruz Biotechnology). To validate the IP procedure, 10% of the sample for IP was used as an "input" (positive control), and chromatin in the presence of normal mouse IgG was used as a negative control. Immunoprecipitated DNA and input DNA were analyzed by qPCR with SsoAdvanced™ Universal SYBR® Green Supermix (Bio-Rad Laboratories, Hercules, CA, USA). Data were analyzed using the delta-delta comparative threshold cycle ($2^{-\Delta\Delta Ct}$) method. Results of qPCR were normalized to input (genomic DNA) and gene desert region (nonspecific binding): ΔCT = (Ct of IP sample − Ct of input − Ct of IgG). Data were expressed relative to positive control (input). PCR primers were designed covering the NF-κB consensus sequences in the promoter region of mouse *Pdgfb* (forward primer 5′-TCCCGATGCCTGTTTAGAT-3′; reverse 5′-TTGCCATCTCTGTGACAGT-3′).

RT-PCR

POCs were incubated with prednisolone 10^{-6}M alone or with either RU486, GRsiRNA, or TNFα or prednisolone 10^{-7}M alone for 24 hours. Total RNA was extracted and subjected to RT-PCR as described.[9] Relative expression was calculated for each gene by the $2^{-\Delta\Delta Ct}$ method, with GAPDH for normalization. The sequences of each primer are as follows: GAPDH: forward 5′-AGGTCGGTGTGAACGGATTTG-3′ and reverse 5′-GGGGTCGTTGATGGCA-ACA-3′; PDGF-BB: forward 5′-ACCCAGAAGACTGTGGATGG-3′ and reverse 5′-CACATT-GGGGGTAGGAACAC-3′.

Western blotting

Western blotting was performed on POC lysates. The cell lysates were centrifuged and separated by 10% SDS-PAGE and transferred onto a polyvinylidene difluoride membrane (Bio-Rad Laboratories). After blocking with 5% BSA in Tris-buffered saline containing 0.05% Tween-20 (TBST), the membrane was incubated with specific primary antibodies at 4°C overnight. The membrane was then washed with TBST and incubated with horseradish peroxidase (HRP)-conjugated secondary antibodies. We detected protein using an enhanced chemiluminescence kit (Thermo Fisher Scientific, Waltham, MA, USA). We used primary antibodies recognizing mouse PDGF-BB (Abcam; Ab23914, 1:500) and GAPDH (Santa Cruz Biotechnology; sc-365062, 1:1000) to determine the protein concentrations in the lysates.

In vitro tube formation assay

Culture media was collected from POC cultures in the presence of prednisolone (10^{-6}M and 10^{-7}M) alone or in addition to RU486 or PDGF-BB neutralizing antibody (Abcam; 1 μg/mL; polyclonal) or RU486 alone. In a separate culture, endothelial progenitor cells (EPCs) were seeded in endothelial progenitor outgrowth cell growth medium (BioChain, Newark, CA, USA; Z7030033). Tube formation assays were performed by using Matrigel Matrix basement membrane (Corning, Corning, NY, USA; 356230) as reported.[9,14] Briefly, 50 μL of Matrigel was added into 96-well culture plates and incubated at 37°C for 30 min to allow the gel to solidify. We then seeded EPCs (2×10^4 cells/well) on polymerized Matrigel in plates and cultured the cells with the collected POC conditioned medium mixed with the endothelial cell culture medium in a ratio of 1:1. Additional controls included PDGF-BB 60 ng/mL (PeproTech, Inc., Rocky Hill, NJ, USA), PBS, PDGF-BB neutralizing antibody, RU486, prednisolone 10^{-6}M or 10^{-7}M, RANKL 60 ng/mL, or M-CSF 30 ng/mL mixed directly into endothelial cell culture medium prior to seeding of EPCs on polymerized Matrigel. After incubation at 37°C for 4 hours, we observed tube formation by microscopy and measured the cumulative tube lengths.

Apoptosis detection assay

Apoptosis detection was performed using an apoptosis detection kit (Abcam; ab176749). Briefly, RAW264.7 cells or mouse bone marrow monocytes plated at a density of 2×10^5 per well in a 96-well microplate were cultured in DMEM or α-MEM with prednisolone concentration of 10^{-7}M and 10^{-6}M were washed, pelted, and resuspended in 200 μL of Assay Buffer. Apopxin Green indicator was added to cells to detect apoptosis, with quantification of fluorescence.

Statistical analysis

All results are presented as mean ± SD. Statistical analysis was performed with analysis of variance (ANOVA) for multiple comparisons and two-tailed Student's *t* tests for comparisons between two groups. Statistical significance was achieved when $p < .05$. For all experiments, *p* values are reported between compared groups as indicated on graphs.

Results

Establishment of young mouse model of GC-induced low bone volume and growth retardation

During skeletal growth, bone mass increases as assessed by bone mineral density and bone size (bone length or height).[25] GCs can impair both processes. In our published model, prednisolone 10 mg/m^2/day impaired bone volume, but not growth.[9] Increasing prednisolone to 20 mg/m^2/day resulted in more significant osteotoxic effects without mortality. A severe osteoporotic bone phenotype was observed in mice receiving prednisolone, as shown by a lower trabecular bone volume in distal femur relative to vehicle controls at 2, 4, and 6 weeks (Fig. 1a). BV/TV, Tb.Th, and Tb.N were decreased, whereas Tb.Sp increased in prednisolone relative to vehicle mice at 2, 4, and 6 weeks (Fig. 1b–e). In regard to growth, both weight and length were decreased in prednisolone relative to

control groups. Changes in size and weight were noted after 2 weeks, but did not reach statistical significance until 4 weeks (Fig. 1f, Supplemental Fig. 1b). Femur length was significantly decreased in prednisolone relative to vehicle groups at 4 and 6 weeks (Fig. 1g,h). Both the proliferative zone and hypertrophic zone in the growth plate play a critical role in endochondral bone formation and long bone elongation.[26] We found the height of the growth plate, specifically the hypertrophic and proliferative zone in prednisolone-treated mice decreased significantly compared to the control group at 2, 4, and 6 weeks (Fig. 1i,j). The height of the resting zone was increased in the prednisolone-treated group at 2 and 4 weeks, but the difference did not persist at 6 weeks relative to control (Fig. 1l). Consequently, the growth plate height in distal femur of the prednisolone group was reduced relative to vehicle controls. Overall, prednisolone 20 mg/m^2/day resulted in a bone phenotype similar to that observed clinically with reduction in bone volume and longitudinal bone growth.

GCs decrease type H vessels, angiogenesis, and osteogenesis

We and others have reported that GCs are associated with a decline in bone vasculature.[7–10] However, how GCs disrupt the steps of angiogenesis/blood vessel maintenance remains unknown. We confirmed that type H vessels were significantly reduced as quantified by length of CD31^{hi}Emcn^{hi} vessels, decreasing by 51%, 21%, and 42% at 2, 4, and 6 weeks, respectively, in prednisolone relative to vehicle mice (Fig. 2a,b). Type H vessels are organized in columns; buds (Fig. 2c, green arrows) extend from columns next to the growth plate and merge to form loops. Elongation of the new buds results in branching of vessels (Fig. 2c, white arrows). We found that budding remained similar after 2 weeks of either prednisolone or vehicle exposure (Fig. 2c, top panel). However, the vessel branch points in prednisolone group decreased significantly relative to vehicle group by 2 weeks. The inhibitory effect on angiogenesis was more severe with Prolonged GC administration, with both decreased budding and vessel branching at 4 and 6 weeks relative to vehicle (Fig. 2c,d). These observations suggest that GCs disrupt type H vessel stabilization/maturation and inhibit bone angiogenesis.

Angiogenesis is coupled with osteogenesis where type H blood vessels and Osx$^+$ osteoprogenitors are found in close proximity.[4,12] As expected, the number of Osx$^+$ osteoprogenitors around type H vessels was significantly reduced by prednisolone administration at 2, 4, and 6 weeks relative to vehicle controls (Fig. 3a,b). Mineral apposition rate (MAR) in the cancellous bone of the distal femurs was significantly decreased after 2 weeks of prednisolone administration and remained low in mice treated for 4 and 6 weeks relative to vehicle (Fig. 3c,d). Taken together, GC administration led to attenuated bone formation that was associated with a decline in type H vessels in trabecular bone adjacent to growth plate.

Excessive GCs decrease preosteoclasts and its synthesis of PDGF-BB

We have previously reported that POCs produced PDGF-BB to couple angiogenesis and osteogenesis during bone modeling and remodeling.[14] In adult glucocorticoid-induced osteoporosis (GIO) mouse models, GCs have been shown to have a biphasic effect on osteoclast bone resorption, with increased resorption in the early phase due to enhanced

survival of osteoclasts, but suppression of bone resorption in the late phase due to GC suppression of osteoclast differentiation.[14,16] To investigate the effect of GCs on osteoclast-mediated coupling of angiogenesis in our young GIO mouse model, we examined the effect of GCs on the number of POCs and synthesis of PDGF-BB. The number of mononuclear $Trap^+$ cells defined as POCs remained similar in trabecular bone in prednisolone mice relative to vehicle control after 2 weeks, and then significantly declined by 4 and 6 weeks (Fig. 4a,b). Immunofluorescence staining showed that the percent of TRAP-positive cells that were also positive for PDGF-BB were decreased in prednisolone-exposed mice relative to vehicle controls as early as 2 weeks and declined further by 4 and 6 weeks (Fig. 4c,d). The concentration of PDGF-BB in both bone marrow and serum was decreased at all time points in prednisolone-exposed mice relative to vehicle control mice points (Fig. 4e,f).

We then cultured mouse bone marrow mononuclear cells and RAW 264.7 cells for POC and osteoclast induction, identified by Trap staining (Fig. 5a). Addition of prednisolone at day 0 of culture resulted in fewer cells secondary to apoptosis at higher concentrations (10^{-6}Mrelative to 10^{-7}M) (Fig. 5a–d). To determine if our prior finding of decreased PDGF-BB in GC-treated mice was due to decreased number of POCs or decreased *Pdgfb* synthesis, we verified that POCs are the major source of PDGF-BB. Consistent with our previous study,[14] POC culture media had the highest PDGF-BB concentration (Fig. 5e). Physiologic endogenous GCs are necessary for the maintenance of whole-body homeostasis, whereas excessive GC concentrations used in medical treatments disrupt homeostasis.[27] To investigate the concentration of GCs that impair PDGF-BB synthesis, we cultured RAW 264.7 cells in RANKL and M-CSF for 3 days, then exposed POCs to various prednisolone concentrations (0, 10^{-9}M, 10^{-8}M,10^{-7}M, 10^{-6}M, or 10^{-5}M) for 24 hours. (Fig. 5f). We found that the prednisolone concentration of 10^{-7}M and 10^{-8}M partially suppressed PDGF-BB synthesis and was further suppressed by even higher concentrations (10^{-6}M and 10^{-5}M) (Fig. 5f). As pharmacologic versus physiologic GCs used clinically are 10-fold higher, we set prednisolone 10^{-6}M as excessive dose and prednisolone 10^{-7}M as control for the remainder of the in vitro experiments. Overall, our results indicate that GCs inhibit PDGF-BB by both decreasing POC numbers and production/secretion of PDGF-BB from POCs.

Excessive GCs suppress POC PDGF-BB transcription via GR/NF-κB signaling pathway

GCs bind to GR, then translocate to the nucleus to regulate gene transcription.[28] The *Pdgfb* promoter region contains a NF-κB binding domain[17,18] and GR is known to regulate NF-κB.[29,30] To explore the mechanism of GC suppression of PDGF-BB in POCs, we examined the affinity of NF-κB (P65) binding to one potential *Pdgfb* promoter site by ChIP assay of POCs and treated with either control (10^{-7}M) or excessive (10^{-6}M) prednisolone (Fig. 6a). TNFα, which can stimulate NF-κB mediated signaling pathway independently of GR, was utilized as a positive control. We verified that TNFα increased PDGF-BB concentration in both a dose-dependent (Fig. 6b) and time-dependent (Fig. 6c) manner. To validate the role of GR in the signaling pathway, we also manipulated GR signaling by using GR siRNA and RU486, a progesterone antagonist that disrupts the GR/NF-κB interaction. GR siRNA effectively blocked GR, whereas control siRNA did not effect GR (Fig. 6d). Excessive prednisolone (10^{-6}M) significantly decreased binding of NF-κB (P65) to the *Pdgfb* promoter (Fig. 6e,f) and PDGF-BB synthesis (Fig. 6g) relative to prednisolone

10^{-7}M control. Addition of GR siRNA, RU486, or TNFα each rescued NF-κB binding to *Pdgfb* promoter in the prednisolone 10^{-6}M group (Fig. 6e,f) and PDGF-BB synthesis (Fig. 6g). Furthermore, relative to control prednisolone, *Pdgfb* transcription (Fig. 6h) and POC PDGF-BB secreted in culture media (Fig. 6i) were decreased in cells exposed to excessive prednisolone, but was rescued with addition of GR siRNA, RU486, or TNFα. Finally, Matrigel tube formation assays with endothelial precursor cells plus POC conditioned-culture media demonstrated robust tube formation with control prednisolone (10^{-7}M) POC-conditioned medium, which was suppressed by antibody against PDGF-BB (Fig. 6j,k). Tube formation was decreased by excessive prednisolone (10^{-6}M) POC-conditioned medium, but was rescued when POCs were co-treated with either TNFα or RU486 relative to control prednisolone (Fig. 6j,k). Interestingly, tube formation was comparable between POC culture media conditions with 10^{-6}M with RU486 and RU486 alone. Direct addition of prednisolone, anti-PDGF-BB, TNFα, RU486, RANKL, or M-CSF alone to endothelial cell culture media did not stimulate endothelial tube formation (Supplemental Fig. 1c,d), further supporting that POCs are a major source of PDGF-BB for endothelial tube formation, synthesis of which is suppressed GR/NF-κB transrepression.

Deletion of *Pdgfb* in Trap$^+$ cells mimics GC effect on bone vasculature

To verify the mechanism in vivo, we generated mice with deletion of *Pdgfb* in Trap$^+$ cells (*Pdgfb*$^{-/-}$). Two-week-old mice were injected intraperitoneally daily with either vehicle or prednisolone (10 mg/m^2/day) for 4 weeks. *Pdgfb*$^{-/-}$ mice showed decreased type H vessels as assessed by vessel length and branching points and vessel-associated osteoprogenitors relative to their *Pdgfb*$^{+/+}$ littermates (Fig. 7a–d). Although prednisolone decreased type H vessels and osteoprogenitors in wild-type mice (Pdgfb$^{fl/fl}$), the effect of prednisolone was abrogated in *Pdgfb*$^{-/-}$ mice (Fig. 7a–d). There was a statistically significant difference in length of type H vessels, branching points, and osteoprogenitors in *Pdgfb*$^{fl/fl}$ mice treated with prednisolone and *Pdgfb*$^{-/-}$ mice, suggesting their prednisolone exposure did not completely suppress PDGF-BB to the level of the knockout mice. Overall, the in vivo studies support that GC transrepression of PDGF-BB is a major contributor to the observed bone vasculature phenotype.

Discussion

GIO affects 30% to 50% of all patients on GC therapy.[31] Although osteotoxic side effects of GCs are observed across the lifespan, children are an exceptionally vulnerable population. Children treated with chronic, high-dose steroids have an equally observed incidence/prevalence of osteoporosis relative to adults, plus impairment of linear growth.[3,32,33] Physiologic cortisol in humans, including children is 5 to 7 mg/m^2/day.[34,35] During times of illness, cortisol levels increase 10-fold to 20-fold (50–100 mg/m^2/day). Because prednisolone is five times more potent than hydrocortisone, the dose utilized in the current manuscript (20 mg/m^2/day) equates to 100 mg/m^2/day of hydrocortisone equivalent. When prednisone and prednisolone are used in children as treatment for medical conditions such as muscular dystrophy, rheumatological conditions, or leukemia, the steroids are dosed on a weight basis, generally 2 mg/kg. Adjusted for metabolic weight by body surface area, the doses equates to 40 to 150 mg/m^2/day of hydrocortisone equivalent. Using a higher dose

of GCs than our previous publication[9] (50 in prior report compared to 100 mg/m^2/day of hydrocortisone equivalent in current report), we established a young mouse model with both low bone volume and impaired growth.

GIO is the result of GC suppression of osteoblast and osteoclast differentiation, induction of osteoblast apoptosis, but survival of osteoclasts.[7,16,36–40] The mechanism of GC-induced growth retardation includes inhibition of chondrocyte differentiation, stimulation of chondrocyte apoptosis, inhibition of the growth hormone (GH)/insulin-like growth factor 1 (IGF-1) axis, and impairment of blood vessel invasion into the growth plate.[41,42] In this study, utilizing our young GIO mouse model, we found that GCs profoundly inhibited type H vessel formation, bone formation, and growth in a dose-dependent and time-dependent manner. Bone mass acquisition impairments preceded longitudinal growth, with a decrease in bone volume noted within 2 weeks of GC exposure, whereas a significant difference in femur length was not noted until 4 weeks of GC relative to vehicle. Further experiments are needed to determine if the growth impairment and bone vasculature changes are dependent or only associations.

During bone modeling and remodeling, endocrine and paracrine factors induce migration and differentiation of progenitor cells to couple angiogenesis and osteogenesis.[43–46] POCs have emerged as an important paracrine source of both angiogenic and osteogenic coupling factors. GCs regulate osteoclast precursor proliferation and differentiation in a dose-dependent manner, such that excessive GCs result in a decreased number of POCs in vitro.[16,38] In our young GIO model, we noted the POCs remained similar after 2 weeks relative to vehicle-treated controls, but decreased after chronic exposure (4 weeks). The decrease in number of type H blood vessels and osteogenesis preceded the decline in POCs, with differences noted by 2 weeks of GC exposure. Therefore, the effect on bone formation may be due to the known direct effects of GCs inducing apoptosis and inhibiting differentiation of osteoblast lineage cells.[37,47]

The growing skeleton is continually modeled and remodeled during which angiogenesis, specifically type H vessels, plays a critical role in osteogenesis and bone growth.[12,13] At the border between the growth plate and primary spongiosa, type H blood vessels invade into the growth plate and provide nutrition as well as the signaling molecules that regulate bone formation and bone growth.[20,48,49] GCs are associated with a decline in bone vasculature,[7–10] but details of the signaling mechanism remain unknown. Type H vessels are organized in columns below the growth plate, interconnected by distal, loop-like arches. Buds extend from the columns in close proximity of growth plate hypertrophic chondrocytes, merging with adjacent buds to form loops.[50] Buds decline in mice by 12 weeks of age, as osteogenesis slows.[50] Our previous study revealed a significant decrease in type H vessels in mice exposed to prednisolone at 4 weeks; however, it did not reflect the dynamic changes of type H vessels in the growing skeleton.[9] In this study, we observed a remarkable suppression of type H vessels in the distal femur of GC-treated mice and this inhibitory effect became more pronounced over 2 weeks to 6 weeks. After 2 weeks of GC administration, the distal type H vessel columns and branching were mainly affected, whereas after 4 and 6 weeks, budding and columns more proximal to the growth plate

decreased relative to vehicle controls. The results suggest that GCs impair type H blood vessel maturation first, and angiogenesis after more chronic exposure.

PDGF-BB has been reported to stimulate migration and angiogenesis of EPCs.[51] We have previously reported that POCs are a major source of paracrine PDGF-BB to recruit endothelial tube cells for the formation of type H blood vessels during bone modeling and remodeling.[14] Our previous study showed a decreased number of PDGF-BB$^+$ Trap$^+$ cells after 4 weeks of GC.[9] In the present study, we found that GC not only decreased POC number, but also PDGF-BB transcription. Controlling for the decreased POC numbers with chronic GC exposure, fewer Trap$^+$ cells were also positive for PDGF-BB as early as 2 weeks of GC exposure. Additionally, we observed decreased PDGF-BB concentration in the bone marrow and serum after 2 weeks of GC exposure, prior to a change in the number of POCs, similar to prior reports of PDGF-BB concentrations in relation to GC in the early phase of wound healing.[52] We confirmed a significantly decreased PDGF-BB concentration in POC cultures in the presence of excessive prednisolone relative to control concentration. Although the *Pdgfb* promoter region does not contain a GC response element, it does have a NF-κB binding domain.[53] Through direct protein–protein interactions, GC/GR heterodimers bind to activated NF-κB and prevent it from binding to κB sites, repressing target gene transcription.[53] We found GCs decreased the binding of NF-κB (P65) to the *Pdgfb* promoter, which resulted in decreased transcription and PDGF-BB expression in POCs (Fig. 8). In vitro, the GR antagonist (RU486), direct knockdown of GR using siRNA, or direct stimulation of NF-κB using TNFα rescued endothelial cell tube formation. Our prior study also showed that inhibition of cathepsin K, a protein produced by mature osteoclasts to dissolve the collagen matrix, increased POC PDGF-BB secretion and prevented GIO in young mice.[9]

POCs are not the only source of PDGF-BB, which is demonstrated in the immunofluorescence staining of PDGF-BB and Trap, because there are also PDGF-BB$^+$ cells that are not positive for Trap (Fig. 4b). Prior reports have shown that activated macrophages and endothelial cells produce PDGF-BB.[14,54] Because the GR is expressed in almost every bone cell,[38,47,55] we suspect that GC may suppress *Pdgfb* transcription by a similar mechanism in other cells types than POCs. In this study, we found that deletion of PDGF-BB in Trap-expressing cells resulted in a similar vasculature phenotype as treatment with GCs. Further studies are needed to evaluate this pathway in other cell types. Additionally, PDGF-BB signaling is not selective for endothelial cells alone. PDGF-BB can directly target the osteoblast lineage, mainly by promotion of osteoprogenitor migration.[56–58] Therefore, the effect on osteoblasts and changes in bone volume may not be due solely to the change in type H vessels, but may also directly impair osteogenesis by decreasing PDGF-BB. Another limitation of the study is that we did not specifically disrupt GR signaling in osteoclasts. There are conflicting reports on the impact of loss of GR in osteoclasts and effects on bone formation,[38,59] which may be due to either the type of GC utilized or differences in genetics of the mouse background strains. Further studies are needed to identify the differences observed in these animal models of direct GCs on osteoclasts on bone formation.

Physiologically, GCs play an important role in maintaining bone modeling and remodeling during which angiogenesis is coupled with osteogenesis. However, excessive and extended exposure of GCs result in alterations of bone cells and angiogenic factors in the microenvironment, and ultimately result in osteoporosis, bone growth retardation, and osteonecrosis. Our findings provide a novel pathological mechanism underlying impairment of bone vasculature in relation to osteotoxic side effects of chronic, high-dose GCs. GCs disrupt angiogenesis and osteogenesis coupling by GR/NF-κB–mediated transrepression of POC PDGF-BB, which was associated with low bone mass and growth retardation in young mice. Recognition of this pathway may help identify novel drug targets to explore potential treatments for GIO, particularly in the growing skeleton.

Supplementary Material

Refer to Web version on PubMed Central for supplementary material.

Acknowledgments

This work was supported by grants from the U.S. National Institute of Arthritis and Musculoskeletal and Skin Diseases, K08-AR064833 (to JC) and R01-AR063943 (to XC).

References

1. Wood CL, Soucek O, Wong SC, et al. Animal models to explore the effects of glucocorticoids on skeletal growth and structure. J Endocrinol. 2018;236(1):R69–91. [PubMed: 29051192]
2. Buckley L, Humphrey MB. Glucocorticoid-induced osteoporosis. N Engl J Med. 2018;379(26):2547–56. [PubMed: 30586507]
3. Hansen KE, Kleker B, Safdar N, Bartels CM. A systematic review and meta-analysis of glucocorticoid-induced osteoporosis in children. Semin Arthritis Rheum. 2014;44(1):47–54. [PubMed: 24680381]
4. Sivaraj KK, Adams RH. Blood vessel formation and function in bone. Development. 2016;143(15):2706–15. [PubMed: 27486231]
5. Kanczler JM, Oreffo RO. Osteogenesis and angiogenesis: the potential for engineering bone. Eur Cell Mater. 2008;15:100–14. [PubMed: 18454418]
6. Saran U, Gemini Piperni S, Chatterjee S. Role of angiogenesis in bone repair. Arch Biochem Biophys. 2014;561:109–17. [PubMed: 25034215]
7. Weinstein RS. Glucocorticoids, osteocytes, and skeletal fragility: the role of bone vascularity. Bone. 2010;46(3):564–70. [PubMed: 19591965]
8. Cui L, Li T, Liu Y, et al. Salvianolic acid B prevents bone loss in prednisone-treated rats through stimulation of osteogenesis and bone marrow angiogenesis. PLoS One. 2012;7(4):e34647. [PubMed: 22493705]
9. Yang P, Lv S, Wang Y, et al. Preservation of type H vessels and osteoblasts by enhanced preosteoclast platelet-derived growth factor type BB attenuates glucocorticoid-induced osteoporosis in growing mice. Bone. 2018;114:1–13. [PubMed: 29800693]
10. Pufe T, Scholz-Ahrens KE, Franke AT, et al. The role of vascular endothelial growth factor in glucocorticoid-induced bone loss: evaluation in a minipig model. Bone. 2003;33(6):869–76. [PubMed: 14678846]
11. Bone GC. Formation of blood vessels in bone maturation and regeneration. Nat Rev Endocrinol. 2014;10(5):250.
12. Kusumbe AP, Ramasamy SK, Adams RH. Coupling of angiogenesis and osteogenesis by a specific vessel subtype in bone. Nature. 2014;507(7492):323–8. [PubMed: 24646994]

13. Ramasamy SK, Kusumbe AP, Wang L, Adams RH. Endothelial notch activity promotes angiogenesis and osteogenesis in bone. Nature. 2014;507(7492):376–80. [PubMed: 24647000]
14. Xie H, Cui Z, Wang L, et al. PDGF-BB secreted by preosteoclasts induces angiogenesis during coupling with osteogenesis. Nat Med. 2014;20(11):1270–8. [PubMed: 25282358]
15. Kusumbe AP, Adams RH. Osteoclast progenitors promote bone vascularization and osteogenesis. Nat Med. 2014;20(11):1238–40. [PubMed: 25375923]
16. Jia D, O'Brien CA, Stewart SA, Manolagas SC, Weinstein RS. Glucocorticoids act directly on osteoclasts to increase their life span and reduce bone density. Endocrinology. 2006;147(12):5592–9. [PubMed: 16935844]
17. Chung CH, Lin KT, Chang CH, Peng HC, Huang TF. The integrin alpha2beta1 agonist, aggretin, promotes proliferation and migration of VSMC through NF-κB translocation and PDGF production. Br J Pharmacol. 2009;156(5):846–56. [PubMed: 19239475]
18. Au PY, Martin N, Chau H, et al. The oncogene PDGF-B provides a key switch from cell death to survival induced by TNF. Oncogene. 2005; 24(19):3196–205. [PubMed: 15735680]
19. Chow EK, O'Connell RM, Schilling S, Wang XF, Fu XY, Cheng G. TLR agonists regulate PDGF-B production and cell proliferation through TGF-beta/type I IFN crosstalk. EMBO J. 2005;24(23):4071–81. [PubMed: 16308570]
20. Hartmann K, Koenen M, Schauer S, et al. Molecular actions of glucocorticoids in cartilage and bone during health, disease, and steroid therapy. Physiol Rev. 2016;96(2):409–47. [PubMed: 26842265]
21. Weinstein RS, Wan C, Liu Q, et al. Endogenous glucocorticoids decrease skeletal angiogenesis, vascularity, hydration, and strength in aged mice. Aging Cell. 2010;9(2):147–61. [PubMed: 20047574]
22. Cheung MC, Spalding PB, Gutierrez JC, et al. Body surface area prediction in normal, hypermuscular, and obese mice. J Surg Res. 2009;153 (2):326–31. [PubMed: 18952236]
23. Dossa T, Arabian A, Windle JJ, et al. Osteoclast-specific inactivation of the integrin-linked kinase (ILK) inhibits bone resorption. J Cell Biochem. 2010;110(4):960–7. [PubMed: 20564195]
24. Xian L, Wu X, Pang L, et al. Matrix IgF-1 maintains bone mass by activation of mtor in mesenchymal stem cells. Nat Med. 2012;18(7): 1095–101. [PubMed: 22729283]
25. Davies JH, Evans BA, Gregory JW. Bone mass acquisition in healthy children. Arch Dis Child. 2005;90(4):373–8. [PubMed: 15781927]
26. Yang L, Tsang KY, Tang HC, Chan D, Cheah KS. Hypertrophic chondrocytes can become osteoblasts and osteocytes in endochondral bone formation. Proc Natl Acad Sci U S A. 2014;111(33):12097–102. [PubMed: 25092332]
27. Ishida Y, Heersche JN. Glucocorticoid-induced osteoporosis: both in vivo and in vitro concentrations of glucocorticoids higher than physiological levels attenuate osteoblast differentiation. J Bone Miner Res. 1998;13(12):1822–6. [PubMed: 9844099]
28. Moutsatsou P, Kassi E, Papavassiliou AG. Glucocorticoid receptor signaling in bone cells. Trends Mol Med. 2012;18(6):348–59. [PubMed: 22578718]
29. Nelson G, Wilde GJ, Spiller DG, et al. NF-kappaB signalling is inhibited by glucocorticoid receptor and STAT6 via distinct mechanisms. J Cell Sci. 2003;116(Pt 12):2495–503. [PubMed: 12734399]
30. Scheinman RI, Gualberto A, Jewell CM, Cidlowski JA, Baldwin AS Jr. Characterization of mechanisms involved in transrepression of NF-kappa B by activated glucocorticoid receptors. Mol Cell Biol. 1995;15(2):943–53. [PubMed: 7823959]
31. Angeli A, Guglielmi G, Dovio A, et al. High prevalence of asymptomatic vertebral fractures in post-menopausal women receiving chronic glucocorticoid therapy: a cross-sectional outpatient study. Bone. 2006;39(2):253–9. [PubMed: 16574519]
32. Hogler W, Ward L. Osteoporosis in children with chronic disease. Endocr Dev. 2015;28:176–95. [PubMed: 26138842]
33. Mattano LA Jr, Sather HN, Trigg ME, Nachman JB. Osteonecrosis as a complication of treating acute lymphoblastic leukemia in children: a report from the Children's Cancer Group. J Clin Oncol. 2000;18(18): 3262–72. [PubMed: 10986059]

34. Paragliola RM, Papi G, Pontecorvi A, Corsello SM. Treatment with synthetic glucocorticoids and the hypothalamus-pituitary-adrenal axis. Int J Mol Sci. 2017;18(10):2201.
35. Alves C, Robazzi TC, Mendonça M. Withdrawal from glucocorticosteroid therapy: clinical practice recommendations. J Pediatr (Rio J). 2008;84(3):192–202. [PubMed: 18535733]
36. Teitelbaum SL. Glucocorticoids and the osteoclast. Clin Exp Rheumatol. 2015;33(4 Suppl 92):S37–9. [PubMed: 26458014]
37. Weinstein RS, Jilka RL, Parfitt AM, Manolagas SC. Inhibition of osteoblastogenesis and promotion of apoptosis of osteoblasts and osteocytes by glucocorticoids. Potential mechanisms of their deleterious effects on bone. J Clin Invest. 1998;102(2):274–82. [PubMed: 9664068]
38. Kim HJ, Zhao H, Kitaura H, et al. Glucocorticoids suppress bone formation via the osteoclast. J Clin Invest. 2006;116(8):2152–60. [PubMed: 16878176]
39. Weinstein RS, Chen JR, Powers CC, et al. Promotion of osteoclast survival and antagonism of bisphosphonate-induced osteoclast apoptosis by glucocorticoids. J Clin Invest. 2002;109(8):1041–8. [PubMed: 11956241]
40. Jia J, Yao W, Guan M, et al. Glucocorticoid dose determines osteocyte cell fate. FASEB J. 2011;25(10):3366–76. [PubMed: 21705669]
41. Smink JJ, Koster JG, Gresnigt MG, Rooman R, Koedam JA, Van Buul-Offers SC. IGF and IGF-binding protein expression in the growth plate of normal, dexamethasone-treated and human IGF-II transgenic mice. J Endocrinol. 2002;175(1):143–53. [PubMed: 12379498]
42. Smink JJ, Gresnigt MG, Hamers N, Koedam JA, Berger R, Van Buul-Offers SC. Short-term glucocorticoid treatment of prepubertal mice decreases growth and IGF-I expression in the growth plate. J Endocrinol. 2003;177(3):381–8. [PubMed: 12773118]
43. Sims NA, Martin TJ. Coupling the activities of bone formation and resorption: a multitude of signals within the basic multicellular unit. Bonekey Rep. 2014;3:481. [PubMed: 24466412]
44. Kular J, Tickner J, Chim SM, Xu J. An overview of the regulation of bone remodelling at the cellular level. Clin Biochem. 2012;45(12): 863–73. [PubMed: 22465238]
45. Del Fattore A, Teti A, Rucci N. Bone cells and the mechanisms of bone remodelling. Front Biosci. 2012;4:2302–21.
46. Peng Y, Wu S, Li Y, Crane JL. Type H blood vessels in bone modeling and remodeling. Theranostics. 2020;10(1):426–36. [PubMed: 31903130]
47. O'Brien CA, Jia D, Plotkin LI, et al. Glucocorticoids act directly on osteoblasts and osteocytes to induce their apoptosis and reduce bone formation and strength. Endocrinology. 2004;145(4):1835–41. [PubMed: 14691012]
48. Gerber HP, Vu TH, Ryan AM, Kowalski J, Werb Z, Ferrara N. VEGF couples hypertrophic cartilage remodeling, ossification and angiogenesis during endochondral bone formation. Nat Med. 1999;5(6):623–8. [PubMed: 10371499]
49. Walzer SM, Cetin E, Grubl-Barabas R, et al. Vascularization of primary and secondary ossification centres in the human growth plate. BMC Dev Biol. 2014;14:36. [PubMed: 25164565]
50. Ramasamy SK, Kusumbe AP, Schiller M, et al. Blood flow controls bone vascular function and osteogenesis. Nat Commun. 2016;7:13601. [PubMed: 27922003]
51. Wang H, Yin Y, Li W, et al. Over-expression of PDGFR-β promotes PDGF-induced proliferation, migration, and angiogenesis of EPCs through PI3K/Akt signaling pathway. PLoS One. 2012;7(2):e30503. [PubMed: 22355314]
52. Beer HD, Fassler R, Werner S. Glucocorticoid-regulated gene expression during cutaneous wound repair. Vitam Horm. 2000;59:217–39. [PubMed: 10714241]
53. Niu F, Yao H, Zhang W. Tat 101-mediated enhancement of brain pericyte migration involves platelet-derived growth factor subunit B homodimer: implications for human immunodeficiency virus-associated neurocognitive disorders. J Neurosci. 2014;34(35): 11812–25. [PubMed: 25164676]
54. Andrae J, Gallini R, Betsholtz C. Role of platelet-derived growth factors in physiology and medicine. Genes Dev. 2008;22(10):1276–312. [PubMed: 18483217]
55. Canalis E, Mazziotti G, Giustina A, Bilezikian JP. Glucocorticoid-induced osteoporosis: pathophysiology and therapy. Osteoporos Int. 2007;18(10):1319–28. [PubMed: 17566815]

56. Gilardetti RS, Chaibi MS, Stroumza J, et al. High-affinity binding of PDGF-AA and PDGF-BB to normal human osteoblastic cells and modulation by interleukin-1. Am J Physiol. 1991;261(6 Pt 1):C980–5. [PubMed: 1767825]

57. Colciago A, Celotti F, Casati L, et al. In vitro effects of PDGF isoforms (AA, BB, AB and CC) on migration and proliferation of SaOS-2 osteoblasts and on migration of human osteoblasts. Int J Biomed Sci. 2009; 5(4):380–9. [PubMed: 23675162]

58. Sanchez-Fernandez MA, Gallois A, Riedl T, Jurdic P, Hoflack B. Osteoclasts control osteoblast chemotaxis via PDGF-BB/PDGF receptor beta signaling. PLoS One. 2008;3(10):e3537. [PubMed: 18953417]

59. Rauch A, Seitz S, Baschant U, et al. Glucocorticoids suppress bone formation by attenuating osteoblast differentiation via the monomeric glucocorticoid receptor. Cell Metab. 2010;11(6):517–31. [PubMed: 20519123]

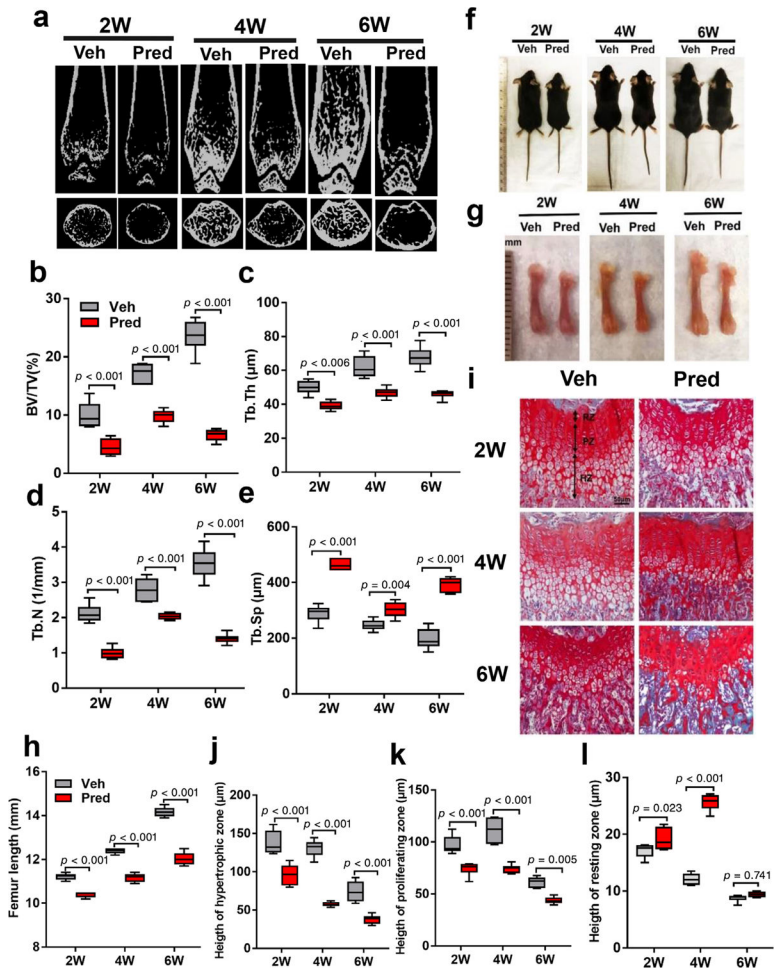

Fig. 1.

Prednisolone impairs bone volume and longitudinal bone growth. (*a*–*e*) Representative microcomputed tomography of mice distal femur after 2, 4, and 6 weeks (2 W, 4 W, and 6 W) of Veh or Pred 20 mg/m^2/day beginning at 2 weeks of age (*a*) and quantitative analysis of trabecular BV/TV (*b*), Tb.N (*c*), Tb.Th (*d*), and Tb.Sp (*e*). (*f*) Images of wild-type mice injected with either Veh or Pred for 2 W, 4 W, or 6 W. (*g*,*h*) Representative photographs of femurs (*g*) and femur length (*h*). (*i*) Safranin orange and fast green staining of distal femoral growth plate. Arrows denote RZ, PZ, and HZ. Scale bar = 50 μm. (*j*–*l*) Quantitative analysis of HZ (*j*), PZ (*k*), and RZ (*l*). $n = 6$ per group. Data are shown as mean ± SD. BV/TV = bone volume per tissue volume; HZ = hypertrophic zone; Pred = prednisolone; PZ = proliferative zone; RZ = resting zone; Tb.N = trabecular number; Tb.Sp = trabecular separation; Tb.Th = trabecular thickness; Veh = vehicle; W = weeks.

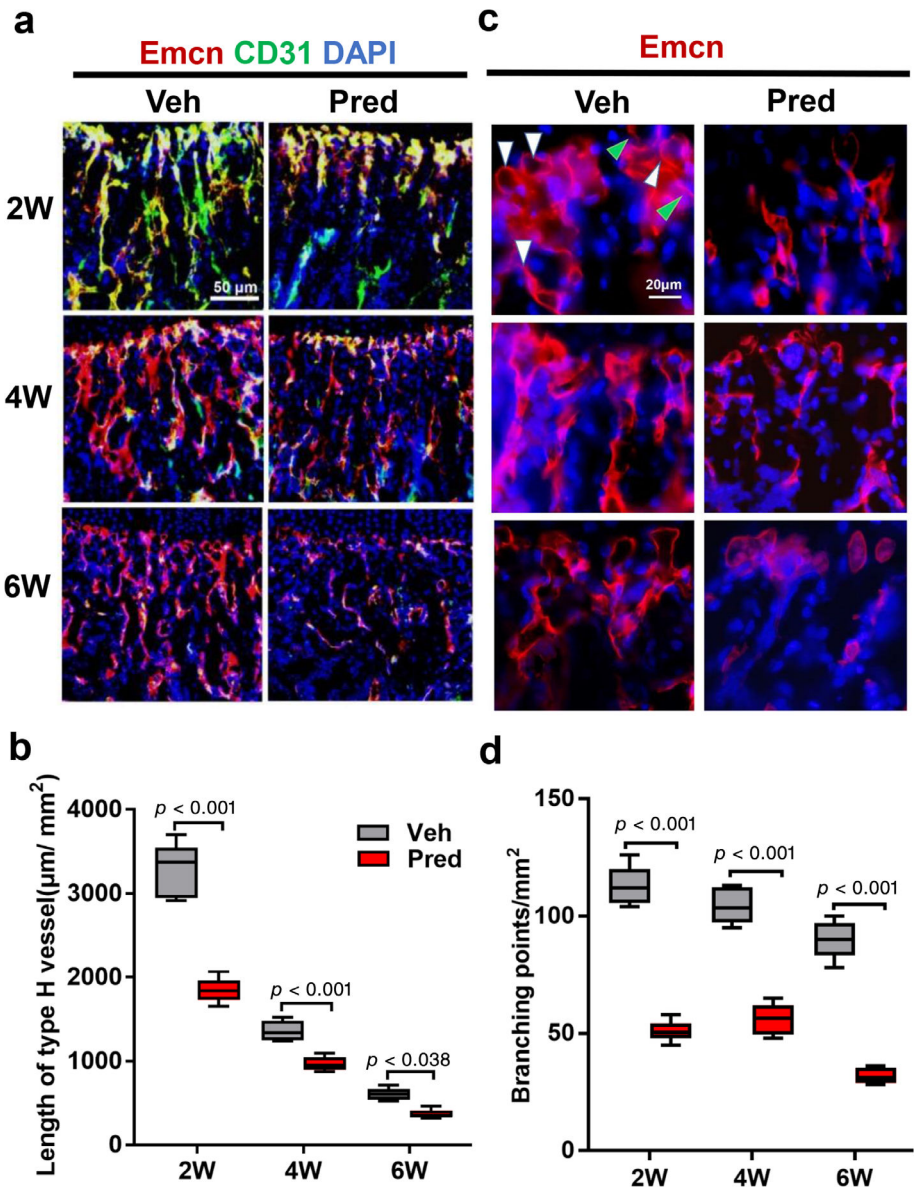

Fig. 2.

Type H vessels are decreased in prednisolone-exposed young mice. (*a,b*) Representative images of Emcn (red) and CD31 (green) immunostaining (*a*) and Emcn alone (*b*) of $CD31^{hi}Emcn^{hi}$ type H vessels (yellow) vessels in distal femur metaphysis of wild-type mice injected with either Veh or Pred 20 mg/m^2/day for 2, 4, or 6 weeks (2 W, 4 W, 6 W). White arrow denotes sprout-like structure; green arrow denotes vessel bud. DAPI stains nuclei blue. Scale bar = 50 μm. (*c,d*) Quantification of length of type H vessel (*c*) and vessel branch points (*d*). $n = 6$ per group. Data are shown as mean ± SD. Pred = prednisolone; Veh = vehicle; W = weeks.

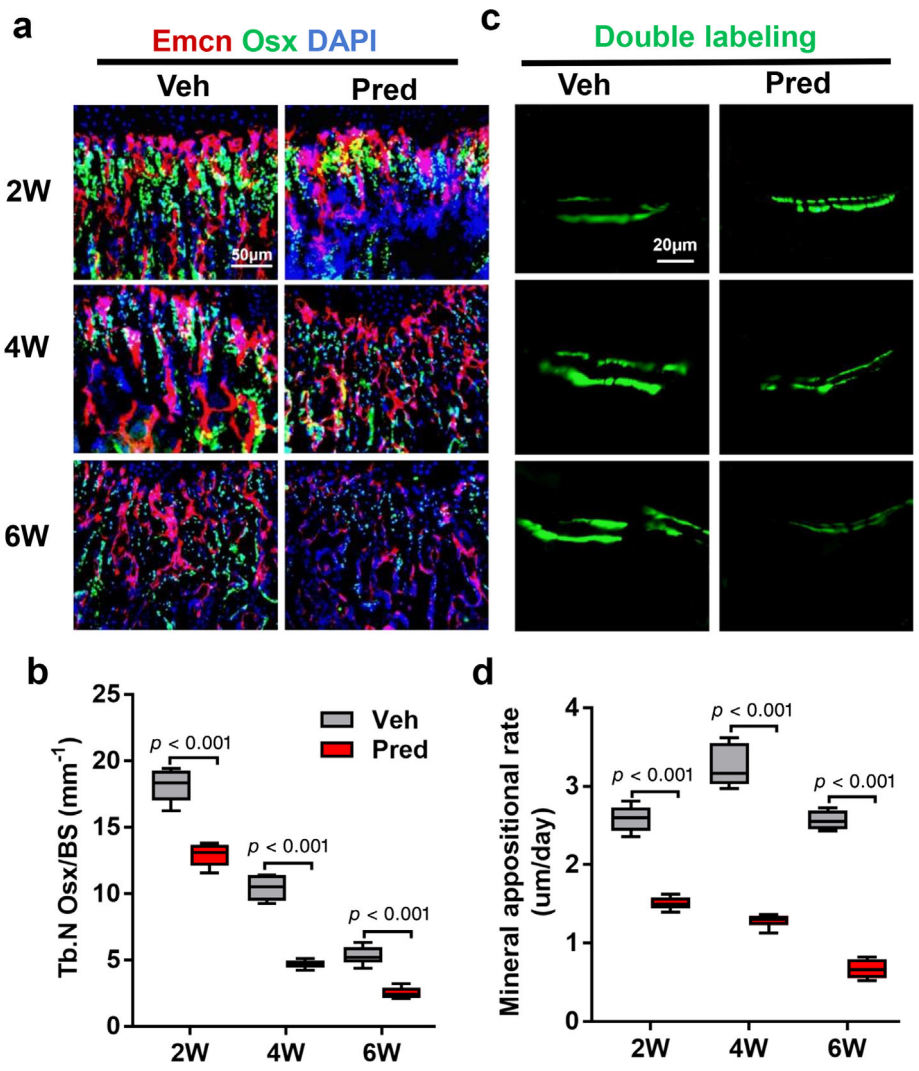

Fig. 3.

Type H vessel associated osteoprogenitors and bone formation are reduced in Pred-treated young mice. (*a*,*b*) Representative images (*a*) and quantification (*b*) of immunostaining of Emcn (red), Osterix-positive (Osx) osteoprogenitors (green), and DAPI (blue) staining of nuclei in distal femur metaphysis in wild-type mice injected with either Veh or Pred 20 mg/m^2/day for 2, 4, or 6 weeks (2 W, 4 W, 6 W). Scale bar = 50 μm. Quantitative analysis reported as N Osx per BS in Tb. (*c*) Calcein double labeling of trabecular bone in distal femur. Scale bar = 20 μm. (*d*) Quantification of MAR. $n = 6$ per group. Data are shown as mean ± SD. BS = bone surface; MAR = mineral apposition rate; N Osx = number of Osx positive cells; Pred = prednisolone; Tb = trabecular bone; Veh = vehicle; W = weeks.

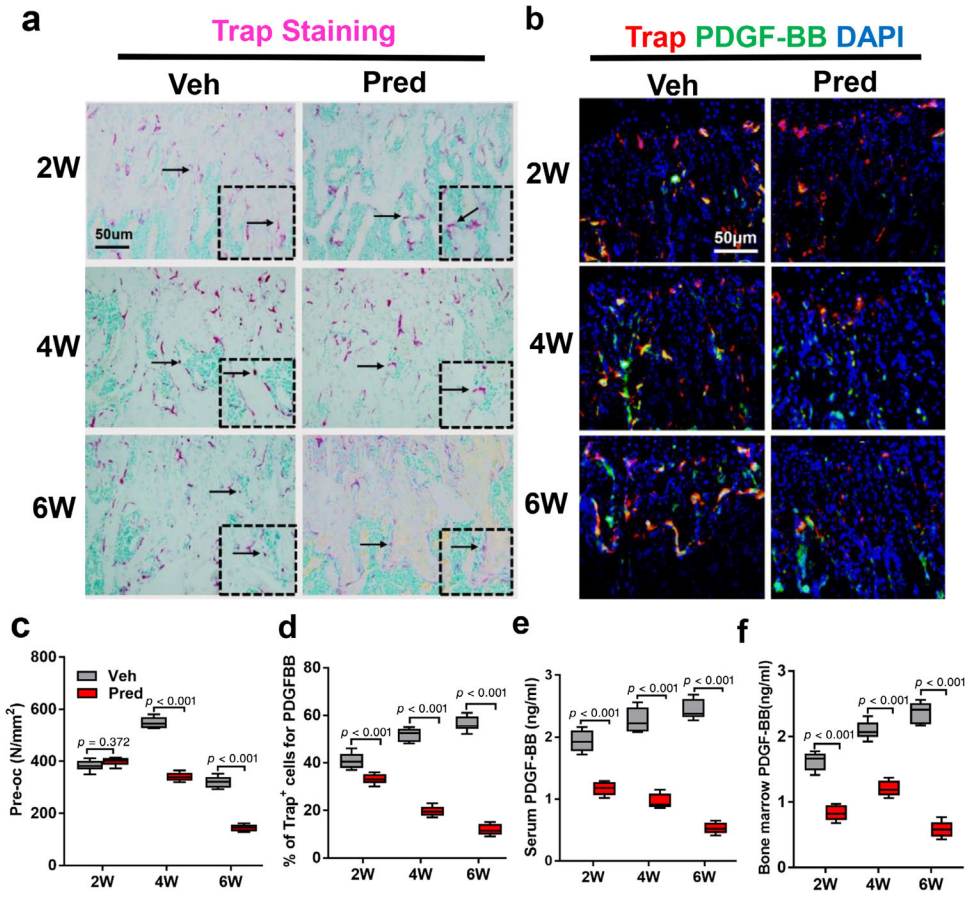

Fig. 4.

PDGF-BB is decreased in Pred-exposed mice. (*a,b*) Representative TRAP staining (magenta) images (*a*) and immunofluorescence images of TRAP (red) and PDGF-BB (green) co-staining (yellow) (*b*) in wild-type mice injected with either Veh or Pred 20 mg/m^2/day Pred for 2, 4, or 6 weeks (2 W, 4 W, 6 W). Methyl green stains nuclei green (*a*) and DAPI (*b*) stains nuclei blue. Scale bar = 50 μm. (*c,d*) Quantitative analysis of the N.POCs on trabecular bone surface (*c*) and percent TRAP$^+$ cells positive for PDGF-BB$^+$ (yellow) in distal femur (*d*). (*e,f*) Serum (*e*) and bone marrow (*f*) PDGF-BB concentration as analyzed by ELISA. $n = 6$ per group (*b*) or $n = 5$ per group (*d*). Data are shown as mean ± SD. N.POCs = number of preosteoclasts; PDGF-BB = platelet-derived growth factor-BB; TRAP = tartrate-resistant acid phosphatase; Veh = vehicle; W = weeks.

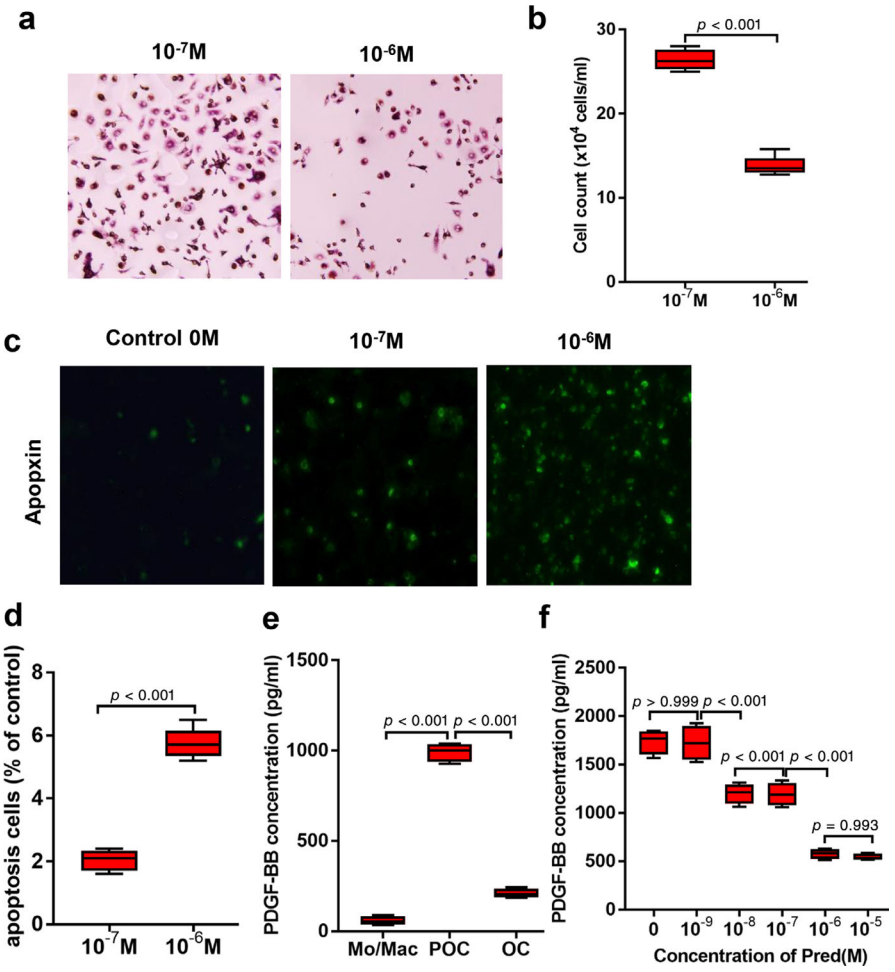

Fig. 5.

Excessive, chronic GCs induce preosteoclast apoptosis and inhibit preosteoclast PDGF-BB synthesis. (*a*,*b*) Representative images of Trap staining of preosteoclasts which were cultured in M-CSF and RANKL with addition of prednisone 10^{-7}M (control) or excessive prednisolone 10^{-6}M for 3 days (*a*) and quantification of number of preosteoclasts (*b*). (*c*,*d*) Cell apoptosis in prednisolone-treated (0M, 10^{-7}M, and 10^{-6}M) preosteoclasts (monocytes after 3 days with addition of M-CSF and RANKL) was assessed by Apopxin Green–positive cells (*c*) and quantification of apoptotic cells (*d*). (*e*) PDGF-BB concentration in culture media of bone marrow monocytes after culture for 0, 3, and 7 days in the presence of M-CSF and RANKL, denoted as Mo/Mac, Pre-OC, and OC, respectively. (*f*) PDGF-BB concentration in culture media of RAW246.7 cells cultured for 3 days with M-CSF and RANKL, with addition of prednisolone (concentration as denoted) for 24 hours after day 3. Assays performed at least four times. Data are shown as mean ± SD. Mo/Mac = monocytes/macrophages; OC = osteoclasts; Pre-OC = pre-osteoclasts.

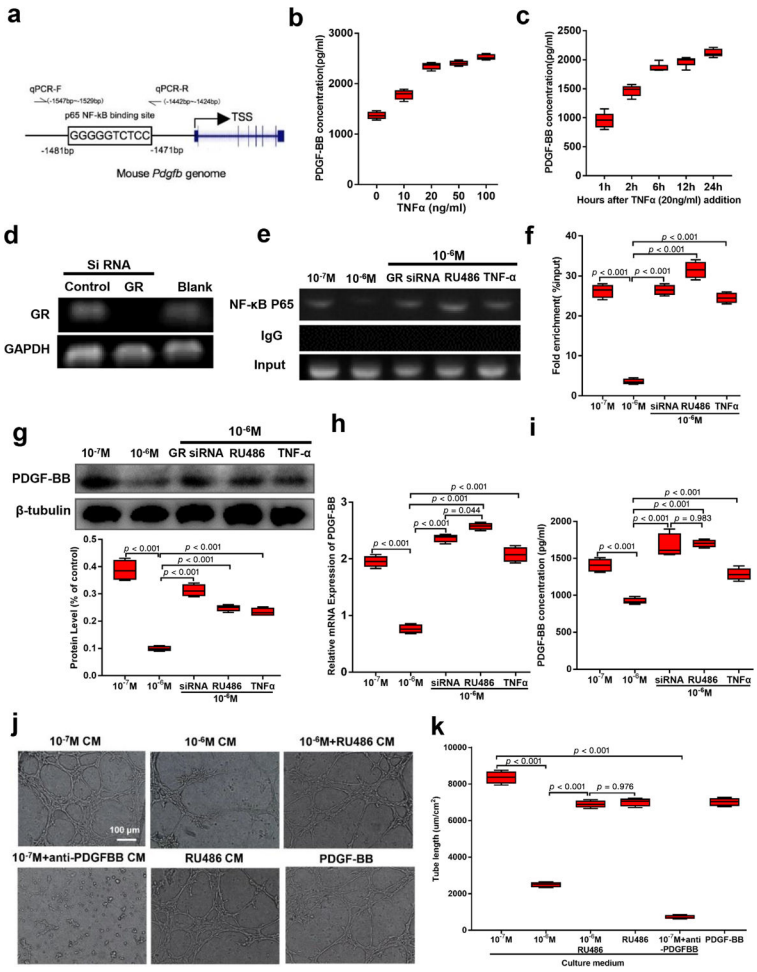

Fig. 6.

Glucocorticoids inhibit preosteoclast PDGF-BB through GR/NF-κB–mediated transrepression. (*a*) Schematic illustration of NF-κB binding site in mouse *Pdgfb* promoter binding sites for p65 NF-κB and PCR primer design strategy for the analysis of ChIP. (*b,c*) PDGF-BB concentrations of mouse bone marrow monocytes and RAW246.7 cells cultured for 3 days in M-CSF and RANKL to form preosteoclasts, followed by stimulation with TNFα at denoted concentrations (*b*) or time after TNFα 20 ng/mL (*c*). (*d*) Immunoblot of GR after transfection of preosteoclasts with siRNA control or siRNA GR. GAPDH serves as control to ensure appropriate loading. (*e,f*) Immunoblot (*e*) and quantification (*f*) of ChIP assay detecting binding activity between p65 subunit of NF-κB and *Pdgfb* promoter using a NF-κB-p65 antibody in preosteoclasts culture plus addition of prednisolone 10^{-7}M, 10^{-6}M alone, or 10^{-6}M plus GR siRNA, RU486 (progesterone antagonist that disrupts the GR/NF-κB interaction), or TNFα. IgG served as negative control, input as positive control. (*g*) Western blot and quantification of PDGF-BB from cultured conditions utilized in CHIP assay. (*h,i*) Quantification of *Pdgfb* mRNA (*h*) and PDGF-BB protein (*i*) concentration by real-time PCR and ELISA, respectively. mRNA normalized to GAPDH. (*j,k*) Representative images (*j*) and tube length (*k*) from Matrigel endothelial tube formation assay with addition of preosteoclast culture media under denoted conditions. Assays performed in triplicate.

Data are shown as mean ± SD. ChIP = chromatin immunoprecipitation; GR = glucocorticoid receptor; PDGF-BB = platelet-derived growth factor type BB.

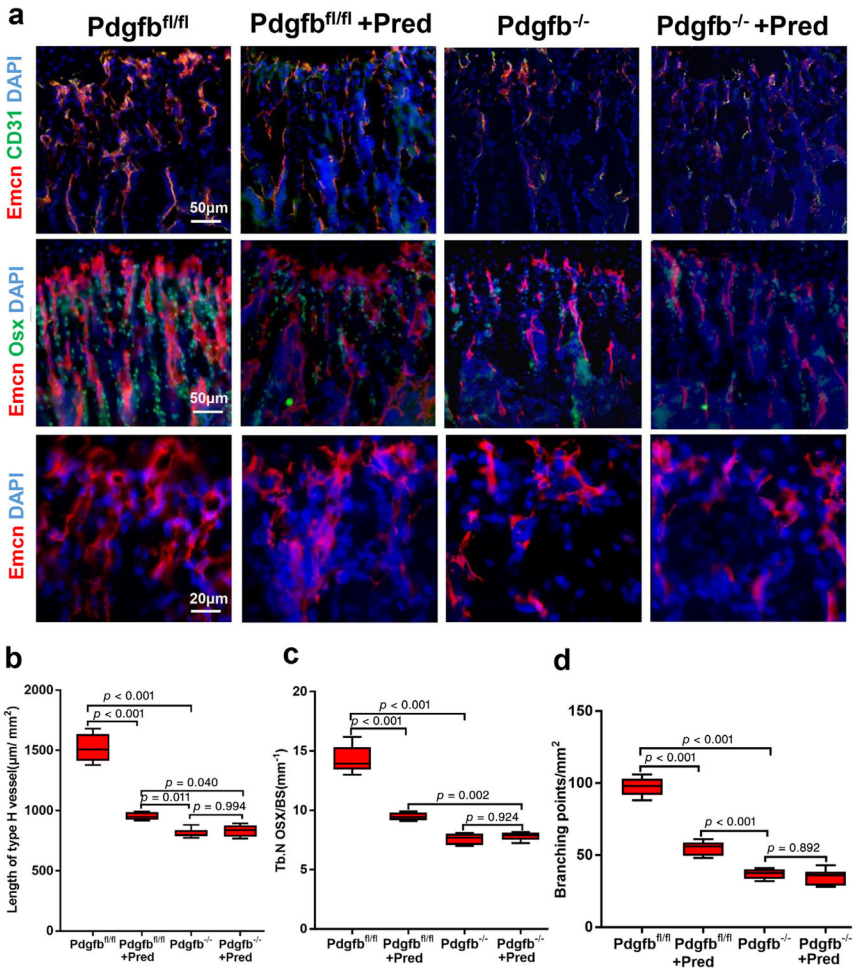

Fig. 7.

Impairment of type H vessel and osteoprogenitors by deletion of *Pdgfb* in Trap^{+} cells is not further reduced by glucocorticoids. (*a*) Representative images of immunofluorescence staining of Emcn (red), CD31 (green), and Osx-positive osteoprogenitors (green) in distal femur metaphysis *Pdgfb*$^{f/f}$ or *Trap-Cre;Pdgfb*$^{-/-}$ (*Pdgfb*$^{-/-}$) mice injected with either vehicle or Pred 10 mg/m^2/day for 4 weeks. DAPI stains nuclei blue. (*b*–*d*) Quantification of CD31^{hi}Emcn^{hi} (yellow) cells (*b*), N Osx per BS in Tb (*c*), and vessel branching points per tissue area (*d*). Scale bar = 50 μm (top and middle panel); 20 μm (bottom panel). *n* = 6 per group. Data are shown as mean ± SD. BS = bone surface; N Osx = number of Osx-positive cells; Osx = Osterix; Pred = prednisolone; Tb = trabecular bone.

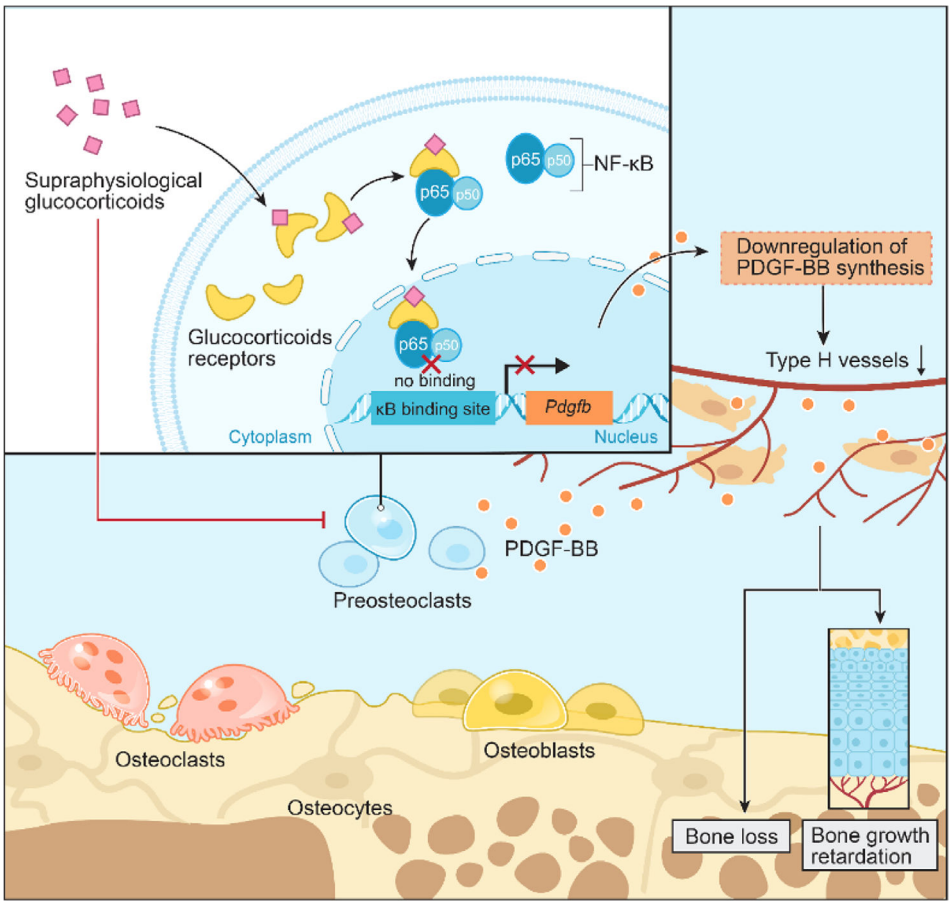

Fig. 8.

Schematic diagram of the genomic effects of GCs on preosteoclasts PDGF-BB secretion. GC binds to the GR in the cytoplasm of preosteoclasts. The GR/GC compounds bind to the p65 subunit of NF-κB and prevents NF-κB nuclear translocation/binding to the κB promoter site of *Pdgfb*, which ultimately leads to downregulation of *Pdgfb* synthesis and PDGF-BB concentration, resulting in less stimulation of type H vessel formation and support of osteogenesis. GR = glucocorticoid receptor; *Pdgfb* = platelet-derived growth factor type B.